33rd Annual International Conference of the IEEE EMBS
Boston, Massachusetts USA, August 30 - September 3, 2011

Local Analysis of Trabecular Bone Fracture

Simone Tassani, Fragiskos Demenegas and George K. Matsopoulos

Abstract—**Assessment of bone fracture risk is the first step in the prevention of traumatic events. In several previous study the use of bone mineral density and bone volume fraction was suggested for the identification of the failure zone, nonetheless the limits of this approach were also investigated, underling the need of other information to fully describe the failure event. In the present study, a comparison between fracture and non-fracture zones of trabecular bone is proposed with the aim of analyze the local structural differences attempting to identify the morphometrical parameters who best can describe the trabecular fracture zone.**

Eighteen trabecular specimens were extracted from the lower limb of two donors without skeletal disorders. All the specimens were scanned by means of a micro-CT and mechanically tested. After the mechanical compression every specimen was scanned again obtaining for every specimen two datasets: pre- and post-failure. An automatic registration scheme, comprising of a three-dimensional automatic registration method to define the differences between the two datasets, and the application of a criterion for defining "broken" or "unbroken" trabeculae, was applied for the identification of the full 3D fracture zone. The morphometrical analysis of fracture and non-fracture zone was performed by the study of several morphometrical parameters, such as bone volume fraction, off-axis angle, structural model index, connectivity density, etc. The results of the two different structures were compared by means of a Wilcoxon non-parametric test.

Ten out of 12 morphometrical parameters were found statistically significantly different between fracture and non-fracture zones, underlining the strong structural difference between the two areas. Nonetheless, only three of them have shown differences superior to 30%, with a reduce overlapping of their distributions: off-axis angle, structural model index and connectivity density. On the other hand, bone volume fraction showed a smaller, even if significant, difference with great overlap of the distributions, in agreement with the limits already pointed out in the literature.

I. Introduction

BONE fracture assessment is a mandatory issue for the prevention of traumatic events and related medical efforts. The standard clinical analysis is based on the estimation of Bone Mineral Density (BMD). Many studies have indicated BMD or structural density, often referred as bone volume fraction (BV/TV), as the principal parameter to determine the tissue mechanical properties [1-4]. However, using only the BMD to identify the individuals who are possible to suffer a fracture is not always reliable [5-7].

The assessment of bone fracture risk using only BMD resulted in errors ranging from 20% to 40% both in *in-vitro* and in clinical studies [8-10], underling the need of other information to fully describe the failure event. A number of specific parameters related to the identification and prediction of a fracture zone (or zones), and of the fracture event in general has been used in both clinical studies [5, 6, 11, 12] and *in-vitro* studies [9, 13-15]. In these *in-vitro* studies, the local analysis of the trabecular structure was studied and compared to the global one in order to identify the weakest point of the structure and, therefore, the fracture zone. The relation of some parameters to the fracture zone was also proposed. The possibility to identify the most significant parameters describing the fracture zone could be of great interest for the prediction of bone fractures, but the extensive analysis of the fracture region was always avoided due to the time-consuming and operator-dependent nature of the visual identification.

The relation of some parameters to the fracture zone was also proposed. The possibility to identify the most significant parameters describing the fracture zone could be of great interest for the prediction of bone fractures, but the extensive analysis of the fracture region was always avoided due to the time-consuming and operator-dependent nature of the visual identification.

A new methodological approach for the automatic identification of trabecular bone fracture zone in micro-CT datasets, after mechanical testing, was proposed in literature and validated against the visual identification of the operators [16].

Aim of the present study is the local analysis of trabecular fracture zone by means of an automatic identification scheme. The comparison of the fracture zone to the unbroken structure was performed with the purpose to identify the main morphometrical differences between fracture and non-fracture zone.

II. Materials & Methods

A. Data Acquisition

Eighteen cylindrical trabecular specimens were extracted from the lower limb of two donors without skeletal disorders during the LHDL (IST-2004-026932) European Project [17]. All the specimens were scanned at a pixel size of 19.5μm by means of a micro-CT (model Skyscan 1072, Skyscan, Kontich, Belgium) and mechanically tested (model Mini

Manuscript received April 26, 2011. This work was supported by the European Community (acronym MOSAIC, project number: PIEF-GA-2009-253924).

The authors are with the Institute of Communication and Computer Systems, 9 Iroon Polytechneiou str., 15780, Athens, Greece

Corresponding author: S. Tassani, phone: +30 210 772 3577; fax: +30 210 772 2468; e-mail: tassani.simone@ gmail.com.

F. Demenegas. e-mail: frankidem@gmail.com.

G. K. Matsopoulos. e-mail: gmatso@esd.ece.ntua.gr.

bionix 858, MTS Systems Corp., Minneapolis, MN, USA) following a previously published protocol [9, 15, 18]. After the mechanical compression every specimen was scanned again in micro-CT obtaining for each one two datasets: pre- and post-failure.

B. Identification of the Fracture and Non-Fracture Zones

An automatic registration scheme for the identification of the full 3D broken region was applied [16].

The used method is a surface-based registration technique which involves the determination and matching of common surfaces of the two sets by the minimization of a distance measure [19]. The method was applied on the pre- and post-failure datasets of every specimen. Analytically, the 3D registration method consists of the followings main steps:

- The application of a segmentation process for the identification of common trabecular surfaces in both sets, which will be then registered.
- The definition of a measure of match (MOM) that quantifies the spatial matching between the pre- and post-failure sets.
- The application of an optimization technique that determines the independent parameters of the transformation model employed, according to the MOM.

The geometrical transformation model employed was the rigid transformation model [20].

The 3D automatic registration method was applied as follows. Based on the assumption that the fracture zone must not pass through the upper and the lower edges of the specimen, two subsets of the post-failure set were initially defined: the upper and the lower subsets, relatively to the fracture zone, consisting of a maximum of 50 contiguous slices. The upper subset was formed from slices of the post-failure set including the first upper slice of the set, up to a randomly selected slice located above the fracture zone. Similar procedure was performed for the identification of the lower subset. Thus, the two subsets clearly correspond to an "unbroken region". Then, the proposed registration method was applied twice: one involving the upper subset of the post-failure dataset with the pre-failure set, and the other the lower subset with the pre-failure set. Consequently, it is expected that the upper and lower subset surfaces, that clearly belong to "unbroken regions", to coincide with the corresponding surfaces of the pre-failure set.

In order to automatically identify the fracture zone on the pre-failure set, every slice was classified as "broken" or "unbroken" according to the following methodology. Every trabecula of every slice of the pre-failure set was identified by a Region of Interest (ROI) and compared to the corresponding ROIs of the registered post-failure set, in order to classify every slice as "broken" or "unbroken". Analytically:

- for every slice of the pre-failure set,
  - for every ROI of the pre-failure set
    - calculate the percentage of overlapping (in pixels) of this ROI with the ROI of the registered post-failure corresponding slice, after the application of the first registration
    - calculate the percentage of overlapping (in pixels) of this ROI with the ROI of the registered post-failure corresponding slice, after the application of the second registration
    - Take the maximum percentage of overlapping (max_over) from both registrations:
      - If the max_over ≥ 30%, ROI is classified as "unbroken"
      - If the max_over < 30%, ROI is classified as "broken"
  - calculate the Broken percentage for this slice of the pre-failure set for all ROIs:

$$Broken\ Percentage = \frac{ROIs\ that\ classified\ as\ "broken"}{all\ ROIs}\ \%$$

The threshold for the classification of each ROI as "broken" or "unbroken" was set to 30%, after experimentation.

Depending on the presence or absence of misaligned ROIs, based on the Broken Percentage criterion, each of the corresponding pre-failure slices was labelled as a "broken slice" or "unbroken slice", respectively. The distribution of misaligned ROIs was computed along the z-axis for the identification of the broken slices and finally a median filter with a width of 0.5mm, corresponding to 25 slices, was applied on this distribution for noise removing. If the Broken Percentage was different from zero, the whole slice was classified as broken. Following the aforementioned criterion, slices identified as broken formed a fracture zone. The result of the Broken Percentage criterion was plotted along the "z" axis, showing the different broken degrees for every slice of the fracture zone. The whole process is summarized in Fig.1.

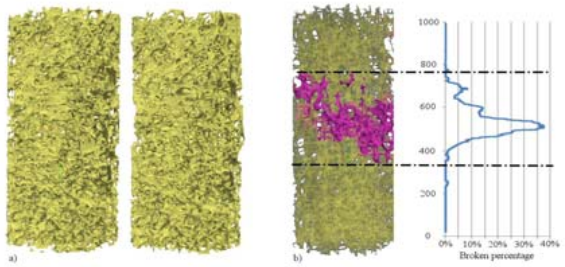

Fig. 1. (a) Pre- and post-failure datasets. (b) Identification of the fracture region by means of the broken percentage identification.

Finally, for every "broken" trabecula an erosion procedure was applied for noise removing (erosion structuring element 3x3 pixels), followed by the application of a dilation procedure (dilation structuring element 75x75 pixels) obtaining for every "broken" trabecula and ellipsoidal Volume of Interest (VOI) centered on each broken trabecula. When VOIs were close enough, they were fused creating a single 3D VOI identifying the fracture zone. The non-fracture zone was identified subtracting the fracture zone

from the whole pre-failure dataset.

C. Morphometrical analysis

Morphometric parameters of the trabecular structure were computed in order to compare the 3D structure of fracture and non-fracture zones in every specimen. For each of the two scenarios, the following parameters were computed: bone volume fraction (BV/TV) [21], bone surface to volume ratio (BS/BV), bone surface density (BS/TV), direct trabecular thickness (Tb.Th*) [22], structure model index (SMI) [23], connectivity density (CD) [24], normalized fabric eigenvalues (H_1, H_2, H_3), computed using the normalisation proposed by Turner et al. [25], off-axis angle [18], degree of anisotropy (DA)[2]. The Broken Volume, defined as the percentage of identified fracture zone volume on the whole dimensions of the specimen was also computed for every specimen. For the calculation of the parameters, the CtAnalyser software was used (CtAnalyser, Skyscan, Kontich, Belgium).

The morphometrical results were statistically compared between fracture and non-fracture zones using a non-parametric paired test (Wilcoxon non-parametric test: differences in parameters were deemed to be statistically significant at a probability of $p<0.05$)

III. Results

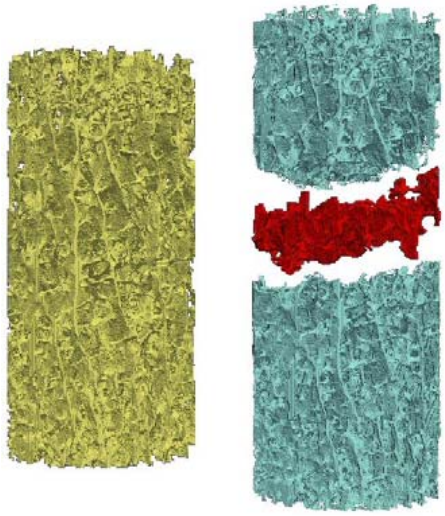

Fig. 2. (a) pre-failure dataset and (b) its decomposition in fracture VOI (red) and non-fracture VOI (light blue) zones.

Fracture and non-fracture zones were identified for every specimen as shown in Fig. 2.

Statistically significant difference between fracture and non-fracture zone was found in ten out of 12 morphometrical parameters. Only BS/TV and H2 showed not statistically significant differences between the two zones. Nonetheless, only 7 parameters had a difference superior to the 10% and only three (SMI, off-axis, DA) superior to 30%. All the results were summarized in Table I.

TABLE I
FRACTURE AND NON-FRACTURE ZONES COMPARISON

Parameter	Fracture	Non-Fracture	Difference %	P values
BV/TV (%)	9.0 (-1.2+4.4)	10.5 (-2.0+4.1)	14%	<0.001*
BS/BV (1/mm)	23.7 (-1.2+5.3)	22.9 (-2.4+2.0)	3%	<0.001*
BS/TV (1/mm)	2.34 (-0.4+0.6)	2.57 (-0.5+0.6)	9%	0.058
Tb.Th (µm)	159 (-22.2+8.6)	163 (-5.7+7.6)	3%	0.020*
SMI	1.87 (-0.3+0.2)	1.42 (-0.4+0.2)	31%	<0.001*
CD	4.57 (-1.7+1.9)	5.25 (-1.4+2.3)	13%	0.035*
H1	0.475 (-0.037+0.031)	0.540 (-0.026+0.041)	12%	0.039*
H2	0.326 (-0.026+0.014)	0.299 (-0.038+0.030)	9%	0.184
H3	0.202 (-0.029+0.018)	0.157 (0.038+0.030)	29%	0.022*
off-axis (°)	82.35 (-3.79+4.36)	8.95 (-2.81+6.79)	820%	<0.001*
DA	2.34 (-0.3+0.6)	3.40 (-0.9+1.1)	31%	0.018*
Broken Volume (%)	7.94	-		-

Comparison in morphometric parameters evaluated for the fracture and non-fracture zones. Median values (- first quartile + third quartile) are reported (Wilcoxon non parametric test, * $p<0.05$).

IV. Conclusions

Aim of the present study was to investigate the morphometrical differences between fracture and non-fracture zone. The biggest part of the analyzed parameters were found statistically significantly different, underlying a strong structural difference between the two analyzed zones. Nonetheless, only few parameters presented a relevant percentage difference.

Many studies have indicated BMD or BV/TV, as the principal parameter to determine the tissue mechanical properties [1-4]. Moreover, BV/TV was also pointed out as the principal parameter describing the local mechanical behavior of trabecular bone [9, 13, 15]. However, a 17% classification error occurred using only BV/TV for the identification of *in-vitro* fracture zone. In the present study BV/TV was found statistically significantly different between fracture and non-fracture zones ($p<0.001$), but the small difference in magnitude is the result of an overlapping of the two distribution, as shown in Fig. 3.

This result mimics the situation reported in several clinical studies where using only the BMD to identify the individuals who are possible to suffer a fracture is not always reliable due to overlapping of the BMD values

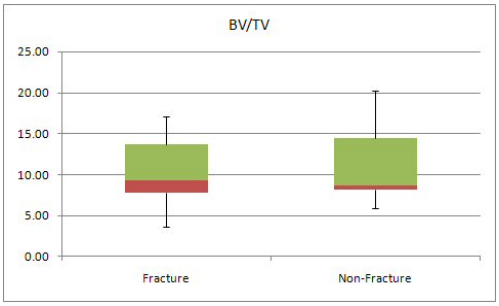

Fig. 3. Box-plot distribution of BV/TV in fracture and non-fracture zone.

between fracture and non-fracture subjects [5-7]. On the other hand a strong difference was reported for the off-axis angle. The influence of this parameter on the mechanical behavior of the trabecular bone was already investigated in

previous studies [15, 18]. The strong difference in the distribution of the off-axis angle in studied zones (Fig. 4.) suggests this parameter to play an important role in the identification and prediction of the trabecular fracture zone.

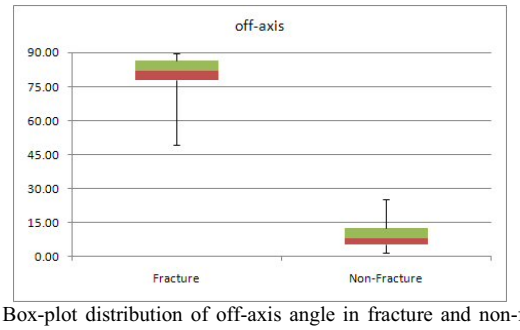

Fig. 4. Box-plot distribution of off-axis angle in fracture and non-fracture zone.

Main limitation of the whole study is the numbers of donors. A wider study must be performed before to generalize the results.

Statistical difference in one parameter cannot be sufficient for the correct prediction of the fracture event. In the present study a set of 12 morphometrical parameters were analyzed. The most of them were found statistically different but only three of them showed a difference superior to the 30% and are therefore suggested for the identification of the trabecular fracture zone. Finally, the broken volume of the fracture region was also computed. In previous studies, where a visual identification was performed, the fracture zone was suggested to involve half of the specimen [9, 13] while in the present study, due to the use of the automatic registration scheme, a smaller fracture region was suggested (8%). This result underline the importance of the local analysis in the study of the trabecular failure event.

ACKNOWLEDGMENT

The datasets were available from http://www.physiomespace.com, and produced by Laboratorio di Tecnologia Medica, Istituto Ortopedico Rizzoli, Bologna, Italy, with the financial support of the EU project LHDL (IST-2004-026932).

REFERENCES

[1] L. J. Gibson, "Biomechanics of cellular solids," *J Biomech,* vol. 38, pp. 377-99, Mar 2005.

[2] R. W. Goulet, S. A. Goldstein, M. J. Ciarelli, J. L. Kuhn, M. B. Brown, and L. A. Feldkamp, "The relationship between the structural and orthogonal compressive properties of trabecular bone," *J Biomech,* vol. 27, pp. 375-89, Apr 1994.

[3] B. D. Snyder, S. Piazza, W. T. Edwards, and W. C. Hayes, "Role of trabecular morphology in the etiology of age-related vertebral fractures," *Calcif Tissue Int,* vol. 53 Suppl 1, pp. S14-22, 1993.

[4] B. Helgason, E. Perilli, E. Schileo, F. Taddei, S. Brynjolfsson, and M. Viceconti, "Mathematical relationships between bone density and mechanical properties: a literature review," *Clin Biomech (Bristol, Avon),* vol. 23, pp. 135-46, Feb 2008.

[5] D. Marshall, O. Johnell, and H. Wedel, "Meta-analysis of how well measures of bone mineral density predict occurrence of osteoporotic fractures," *BMJ,* vol. 312, pp. 1254-9, May 18 1996.

[6] B. R. McCreadie and S. A. Goldstein, "Biomechanics of fracture: is bone mineral density sufficient to assess risk?," *J Bone Miner Res,* vol. 15, pp. 2305-8, Dec 2000.

[7] G. J. Kazakia, A. J. Burghardt, T. M. Link, and S. Majumdar, "Variations in morphological and biomechanical indices at the distal radius in subjects with identical BMD," *J Biomech,* vol. 44, pp. 257-66, Jan 11 2011.

[8] H. Jin, Y. Lu, S. T. Harris, D. M. Black, K. Stone, M. C. Hochberg, and H. K. Genant, "Classification algorithms for hip fracture prediction based on recursive partitioning methods," *Med Decis Making,* vol. 24, pp. 386-98, Jul-Aug 2004.

[9] E. Perilli, M. Baleani, C. Ohman, R. Fognani, F. Baruffaldi, and M. Viceconti, "Dependence of mechanical compressive strength on local variations in microarchitecture in cancellous bone of proximal human femur," *J Biomech,* vol. 41, pp. 438-46, 2008.

[10] J. J. Christopher and S. Ramakrishnan, "Assessment and classification of mechanical strength components of human femur trabecular bone using texture analysis and neural network," *J Med Syst,* vol. 32, pp. 117-22, Apr 2008.

[11] M. G. Donaldson, L. Palermo, J. T. Schousboe, K. E. Ensrud, M. C. Hochberg, and S. R. Cummings, "FRAX and Risk of Vertebral Fractures: The Fracture Intervention Trial (FIT)," *J Bone Miner Res,* May 6 2009.

[12] N. B. Watts, B. Ettinger, and M. S. LeBoff, "FRAX facts," *J Bone Miner Res,* vol. 24, pp. 975-9, Jun 2009.

[13] A. Nazarian, M. Stauber, D. Zurakowski, B. D. Snyder, and R. Muller, "The interaction of microstructure and volume fraction in predicting failure in cancellous bone," *Bone,* vol. 39, pp. 1196-202, Dec 2006.

[14] A. Nazarian, D. von Stechow, D. Zurakowski, R. Muller, and B. D. Snyder, "Bone volume fraction explains the variation in strength and stiffness of cancellous bone affected by metastatic cancer and osteoporosis," *Calcif Tissue Int,* vol. 83, pp. 368-79, Dec 2008.

[15] S. Tassani, C. Ohman, M. Baleani, F. Baruffaldi, and M. Viceconti, "Anisotropy and inhomogeneity of the trabecular structure can describe the mechanical strength of osteoarthritic cancellous bone," *J Biomech,* vol. 43, pp. 1160-6, Apr 19 2010.

[16] S. Tassani, P. A. Asvestas, G. K. Matsopoulos, and F. Baruffaldi, "Automatic identification of trabecular bone fracture," Chalkidiki, Greece, 2010, pp. 296-299.

[17] S. Tassani, C. Ohman, F. Baruffaldi, M. Baleani, and M. Viceconti, "Volume to density relation in adult human bone tissue," *J Biomech,* Sep 15 2011.

[18] C. Ohman, M. Baleani, E. Perilli, E. Dall'Ara, S. Tassani, F. Baruffaldi, and M. Viceconti, "Mechanical testing of cancellous bone from the femoral head: experimental errors due to off-axis measurements," *J Biomech,* vol. 40, pp. 2426-33, 2007.

[19] G. K. Matsopoulos, K. K. Delibasis, N. A. Mouravliansky, P. A. Asvestas, K. S. Nikita, V. E. Kouloulias, and N. K. Uzunoglu, "CT-MRI automatic surface-based registration schemes combining global and local optimization techniques," *Technol Health Care,* vol. 11, pp. 219-32, 2003.

[20] P. A. van den Elsen, E. J. D. Pol, and M. A. Viergever, "Medical image matching-a review with classification," *IEEE Engineering in Medicine and Biology Magazine,* vol. 12, pp. 26-39, 1993.

[21] A. M. Parfitt, M. K. Drezner, F. H. Glorieux, J. A. Kanis, H. Malluche, P. J. Meunier, S. M. Ott, and R. R. Recker, "Bone histomorphometry: standardization of nomenclature, symbols, and units. Report of the ASBMR Histomorphometry Nomenclature Committee," *J Bone Miner Res,* vol. 2, pp. 595-610, Dec 1987.

[22] T. Hildebrand and P. Ruegsegger, "A new method for the model-independent assessment of thickness in three-dimensional images," *Journal of Microscopy,* vol. 185, p. 67, 1997.

[23] T. Hildebrand and P. Ruegsegger, "Quantification of Bone Microarchitecture with the Structure Model Index," *Comput Methods Biomech Biomed Engin,* vol. 1, pp. 15-23, 1997.

[24] A. Odgaard and H. J. Gundersen, "Quantification of connectivity in cancellous bone, with special emphasis on 3-D reconstructions," *Bone,* vol. 14, pp. 173-82, Mar-Apr 1993.

[25] C. H. Turner, S. C. Cowin, J. Y. Rho, R. B. Ashman, and J. C. Rice, "The fabric dependence of the orthotropic elastic constants of cancellous bone," *J Biomech,* vol. 23, pp. 549-61, 1990.